

Temperature Gradient Impact on Heat Exchanger Leaks Using CFD Analysis

Abdulrahman A. Khateeb¹, Abdullah M. Alqahtani¹, Papa Cisse¹, Mohammed A. Alhajri¹,
Dilip Maniar², Carlos F. Lopez², Vishal Nayyar²

¹Saudi Aramco, ²Stress Engineering Services

¹Dhahran 31311, Saudi Arabia; ²Houston, Texas 77041-1101, USA

abdulrahman.khateeb.89@gmail.com; abdullah.qahtani.72@aramco.com; papa.cisse@aramco.com;
mohammed.alhajri.22@aramco.com; dilip.maniar@stress.com; carlos.lopez@stress.com;
vishal.nayyar@stress.com

Abstract – Heat exchanger leaks are common failures in gas and oil industry. However, the root causes of failure are not always obvious to identify. Therefore, utilizing advanced analysis tools such as computational fluid dynamics and finite element analysis are vital to better understand the problem. Here, we discuss a real case of a heat exchanger facing repeated leaks in an oil and gas industry. Detailed computational fluid dynamics analysis is used to determine the impact of temperature gradient on displacement of the heater flanges and gaskets. The simulated conditions include 5 steady-state and transient operating conditions. The analysis results show that thermal expansion cause loss of bolt load and further reduces gasket contact pressure. Maximum gasket scuffing due to differential radial thermal expansion could result in gasket damage over repeated thermal cycles. This finding is the most likely root cause of the repeated heater leaks. The results discuss additional potential root causes of the leaks mainly related to gasket damage due to thermal expansion behavior. The results of this work will be used for future work utilizing finite element analysis tools.

Keywords: Heat Transfer, Thermal Expansion, Oil & Gas, Gasket

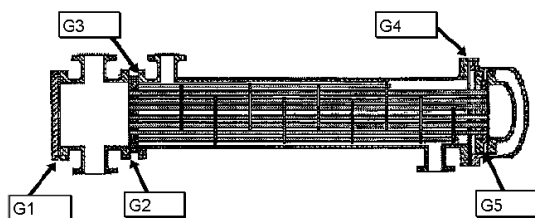
1. Introduction

Heat exchanger equipment are widely used in oil and gas industry to transfer heat from one feed to another [1-2]. There are different types of heat exchangers classified in TEMA code, international standards for heat and tube heat exchangers [3]. These exchangers sometimes fail for several reasons such as excessive operation conditions. Understanding the root causes of such failures may require computational fluid dynamics (CFD) analysis [4-5].

This paper shows real case of a heat exchanger failure where CFD was performed to tackle the issue. The subjected heat exchanger is used to raise the temperature of regen gas in the shell side by circulating hot oil in the tube side. The exchanger operates in a cyclic mode. The gas is heated for a couple of hours and then cut to zero, while the hot oil is running in the tube side. The heating and cooling cycle is repeated about every eight hours.

The exchanger experienced leaks from the shell to tube sheet gasket and at the shell cover gasket. A fugitive gas leak was observed, similar failures were previously observed [6-7]. After removing the insulation, it was confirmed that the shell to tube sheet (G3) – (Gas Side) gasket was leaking and the tube sheet to channel head (G2) – (Hot Oil Side) gasket had minor accumulation of hot oil at the flange. Figure 1 shows these gasket locations on the heater. Furthermore, during the cooling stage an additional leak at the shell cover to shell (G4) gasket was observed. In addition, the gaskets G2 & G3 were displaced from the flanges.

The main objective of the paper is to find out the impact of temperature gradient on the shell of the heat exchanger using CFD analysis. The CFD analysis was performed for two (2) steady-state operating scenarios and for three (3) worst-case transient scenarios. The CFD analysis was performed to understand the impact of thermal gradient on root causes of the leaks.



- Legend:** Gasket Locations Identified by "G" Number
- G1 Represents Channel to Channel Cover Gasket
 - G2 Represents Channel to Fixed Tubesheet Gasket
 - G3 Represents Fixed Tubesheet to Shell Gasket
 - G4 Represents Shell Cover to Shell Gasket
 - G5 Represents Floating Head Cover to Floating Tubesheet Gasket

AHMED.ALSEUD

Fig. 1: General Arrangement of a Single Heater and Gasket Locations

2. Methods

Detailed CFD analysis is used to determine local wall temperatures of the shell surfaces in a heat exchanger. These local temperature gradients are important as they will significantly influence local thermal expansion near the flanges of interest. The fluid temperatures and pressures from analytical calculations along with the rate of heat transfer between the tube and shell-sides of the heat exchanger are used as inputs into the CFD model.

To calculate the local temperature field, the CFD model discretizes and solves the Navier-Stokes equations in the fluid domains. These equations describe the fluid flow and heat transfer using the concepts of conservation of mass, momentum, and energy, with the ideal gas law equation of state used to relate temperature and pressure of the shell-side gas [4]. The following sections detail the modelling inputs and assumptions used along with the analysis results.

2.1. Geometry and Mesh

The internal fluid volume of the tube and shell side was modelled using ANSYS SpaceClaim, as shown in Fig. 2 (left) based on the provided heater drawings. The internal features of the heat exchanger including partition plates, baffles, and impingement plates are modelled as zero-thickness surfaces. The floating head is modelled explicitly as a solid body to capture the conduction heat transfer through its thickness and between the internal oil and the surrounding gas. Gasket grooves were not included as they do not impact shell temperatures significantly. The heat exchanger geometry was discretized using a hybrid tetrahedral/hexahedral mesh, with refinement in small gaps and to resolve curvature, as shown Fig. 2 (right). The resulting mesh contains 5.1 million elements per heat exchanger.

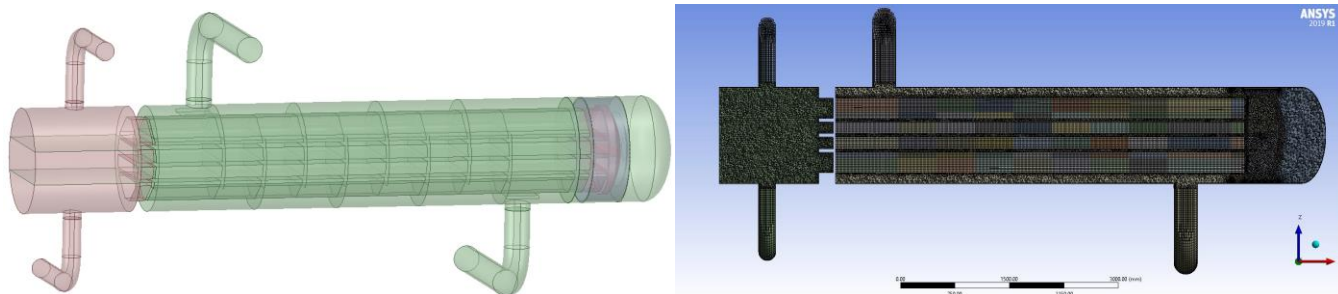


Fig. 2: CFD solution domain of tube and shell side fluids with floating head solid (left), section view of numerical mesh (right).

2.2. Modelling Inputs and Assumptions

Inlet mass flow rate and outlet pressure boundary conditions were used on the tube- and shell-sides of the model to simulate flow conditions. The flow temperatures at these boundaries were determined from the previous analytical thermal calculations. The fluid and thermal properties of the oil and gas are functions of temperature and calculated from real process data and the ideal gas law. Temperature dependent steel and insulation properties are also used. On exterior boundaries, a convection thermal boundary condition was used to model ambient conditions with an additional heat transfer resistance to account for the steel and insulation thickness.

Additional simplifying assumptions were made to streamline the modelling process and improve the convergence of the model. For instance, the tubes are not explicitly modelled and are instead accounted for as four tube bundles with characteristic cross-flow pressure drop and volumetric heat transfer rates determined from the analytical heat transfer calculations. This is needed as explicitly modelling all 532 tubes with the necessary mesh resolution is impractical.

The CFD model was developed using ANSYS Fluent, wherein the Navier-Stokes equations are discretized and solved using an iterative approach. The steady-state solution for the normal operating conditions was solved first and served as the initial condition for the subsequent transient cooling conditions. The effects of turbulence were simulated using the standard k-epsilon model which is a Reynolds Averaged Navier Stokes (RANS) method commonly used for such applications [4]. To capture the effects of the viscous and thermal boundary layer near to the shell walls, standard wall functions were used.

3. Results and Discussion

3.1. Normal Operating Conditions

Figure 3 shows the flow pathlines through the tube- and shell-sides of the model, colored by velocity magnitude. Tube-side flow enters on the top left and exits on the bottom left, with flow also simulated inside the floating head. Shell-side flow enters from the bottom right and exists the top left after winding around the 8 mixing baffles and the tube bundles. Some low velocity flow also enters the right side of the shell by passing over the narrow support baffle and floating head gaps. The gas flow enters the heat exchanger at a velocity of approximately 9.1 m/s (30 ft/s) and increases to a peak velocity of 18.2 m/s (59.7 ft/s) as it exits the shell side, accelerated from the constriction of the impingement plate and from the increased flow temperature.

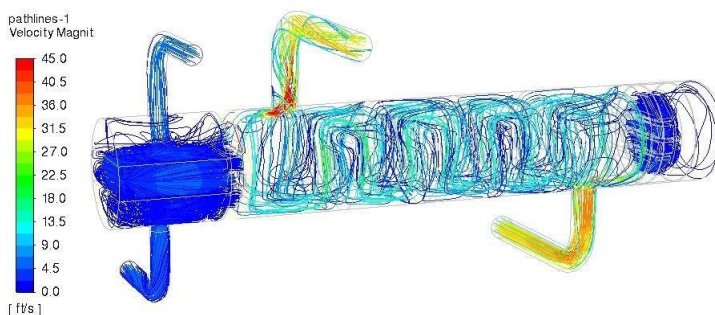


Fig. 3: Pathlines showing velocity magnitude through normal operation of the heat exchanger

Figure 4 shows the same pathlines shown in Fig. 3, but with the color corresponding to temperature. As the shell side flow moves around the baffles and through the tube bundle, it is heated from approximately 249 °C to 285 °C (480 °F to 545 °F). This outlet temperature is consistent with analytical heat transfer calculations and real process data. The centre of the tube bundle has higher gas temperatures as the flow has to slow down to move through the tube bundle, allowing for greater heat transfer. Also, the relatively stagnant flow on the right side of the support baffle allows for significant heat transfer to the gas around the tube bundle and the floating head. Figure 5 shows the resulting wall temperatures. There are significant temperature gradients in proximity to the G2, G3, and G4 flanges even in this steady-state condition.

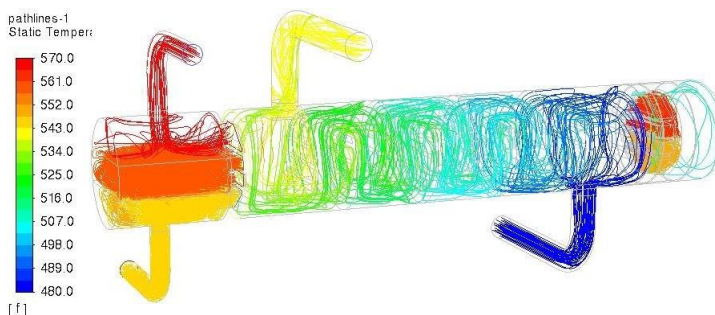


Fig. 4: Pathlines showing temperature magnitude through normal operation of the heat exchanger

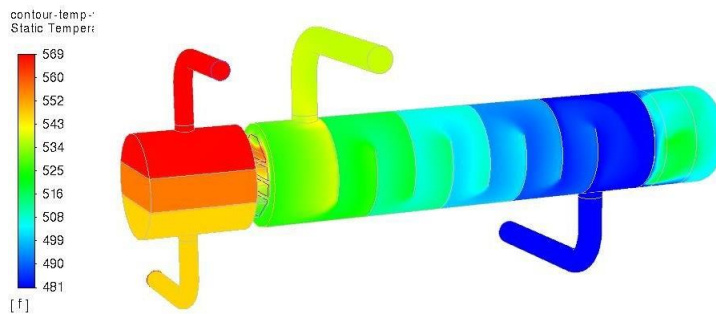


Fig. 5: Wall temperature contour for the normal operation

3.2. Design Conditions

The simulations were repeated for the design conditions, where the inlet temperatures, pressures, and flow rates are different than the normal operating conditions. As the shell side flow passes through the heater, it is heated from approximately 243 °C to 280 °C (469 °F to 535 °F). This outlet temperature is consistent with the analytical heat transfer calculations and the provided process data. The temperature cross-section through the centerline of the heater was analysed. The center of the tube bundle has higher gas temperatures than in the normal operating case. The stagnant flow on the right side of the support baffle is heated by the floating head more in the design condition than in the normal operating condition. Figure 6 shows the resulting wall temperatures for design conditions. The thermal gradients at the G2 and G3 flanges are very similar to the normal operating case, but the gradient at the G4 and G5 flanges are significantly higher than in the normal operating case, due to the change in process conditions.

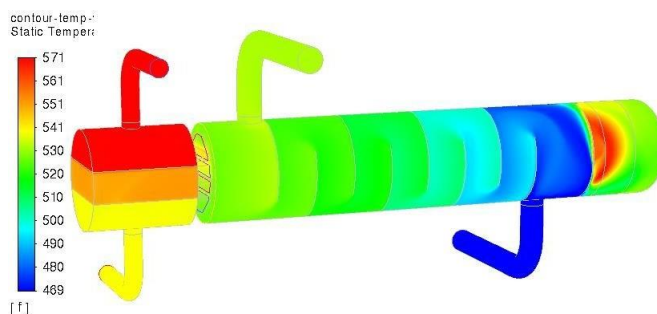


Fig. 6: Wall temperature contour for design conditions

3.3. Transient Normal to Gas Stagnant

The thermal transient between normal operating conditions and gas stagnant conditions was simulated as a shut-in on the shell side occurring over the first 30 seconds and with a 12:1 turndown in tube-side flow rate over 15 minutes. Figure 7 shows the wall temperatures at various timesteps in the transient, starting at t=1s, then 30s, 180s, and 1800s. As the gas valve is closed, gas temperature rises quickly due to the reduced gas flow rate, allowing for the tubes to heat less mass per second. When the gas valve is fully closed (30s) the gas continues to heat further as the tubes are still providing significant heat transfer which is still greater than the shell losses. However, as the tube-side flow rate is reduced, the amount of oil-to-gas heat transfer continues to decrease until shell losses overtake it, resulting in a slow decrease in gas temperature and slight increase in oil temperature due to the reduced heat transfer to the gas.

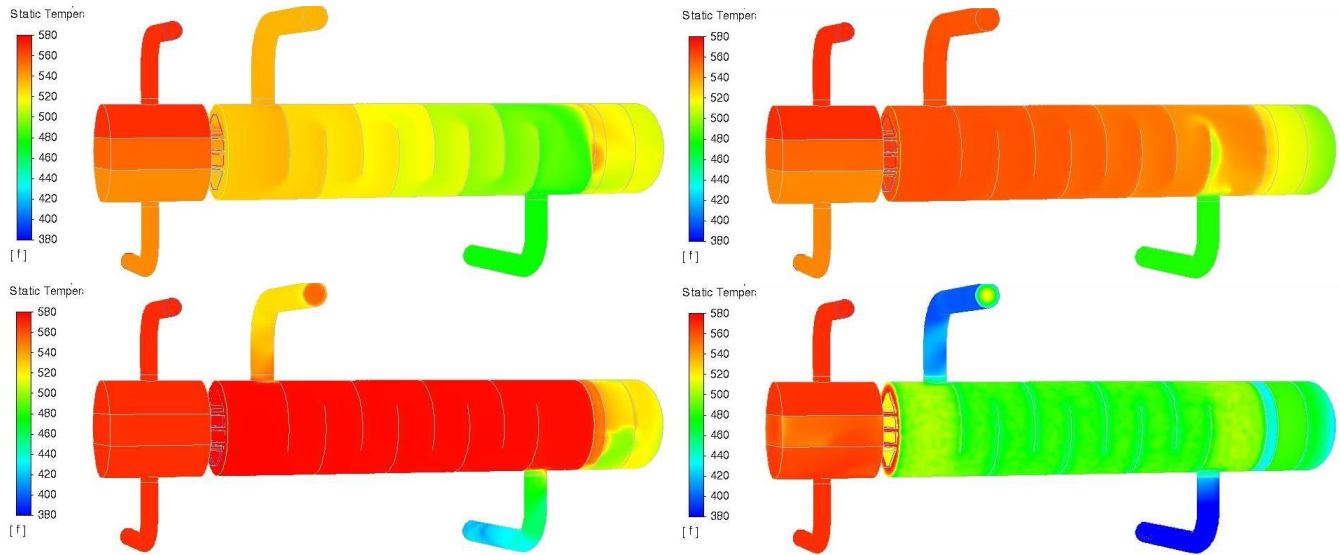


Fig. 7: Wall temperature contour for transition from normal operation to gas stagnant condition at (a) 1 second, (b) 30 seconds, (c) 180 seconds, and (d) 1800 seconds. Temperature ranges from approximately 193 °C to 305 °C (380 °F to 580 °F).

3.4. Transient Normal to Gas/Oil Stagnant

The transient from normal operating conditions to gas and oil stagnant conditions is identical to the normal to gas stagnant case in the first 930 seconds. After that, the tube flow rate continues to reduce to zero, resulting in a similar wall temperature profile to the gas stagnant case but with a significant difference in tube-side temperatures, shown in Fig. 8. This difference is due to the no-flow condition on the tube-side and subsequent heat loss through the insulation. The gas/oil stagnant case results in lower thermal gradients in the G2 and G3 flanges than in the gas stagnant case.

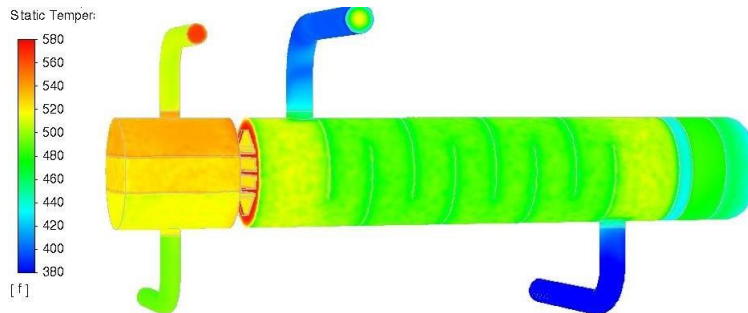


Fig. 8: Wall temperature contour for transition from normal operation to gas stagnant condition at 1800s. Temperature ranges from approximately 193 °C to 305 °C (380 °F to 580 °F).

3.5. Transient Heating (Gas Stagnant to Normal Operation)

The transient heating condition starts with the final time step of the stagnant gas condition and transitions to normal operation. This is simulated as first opening the gas valve over 30 seconds and then increasing the oil flow rate from the 12:1 turndown rate to full rate over 15 minutes. At the moment when the gas valve starts to open, low temperature gas rushes into the shell, replacing the warm stagnant gas. This low temperature gas is then quickly heated by the tube bundle in the first 10-15 seconds of gas flow and then decreases in temperature somewhat when gas flow reaches the maximum rate at 30 seconds due to the higher flow enthalpy. Figure 9 shows the wall temperature contour at 1, 15, 30, and 930 seconds when the tube flow has been restored to normal operating flow. The tube-side temperature reflects the expected temperature drop due to heat transfer from the tubes to the gas.

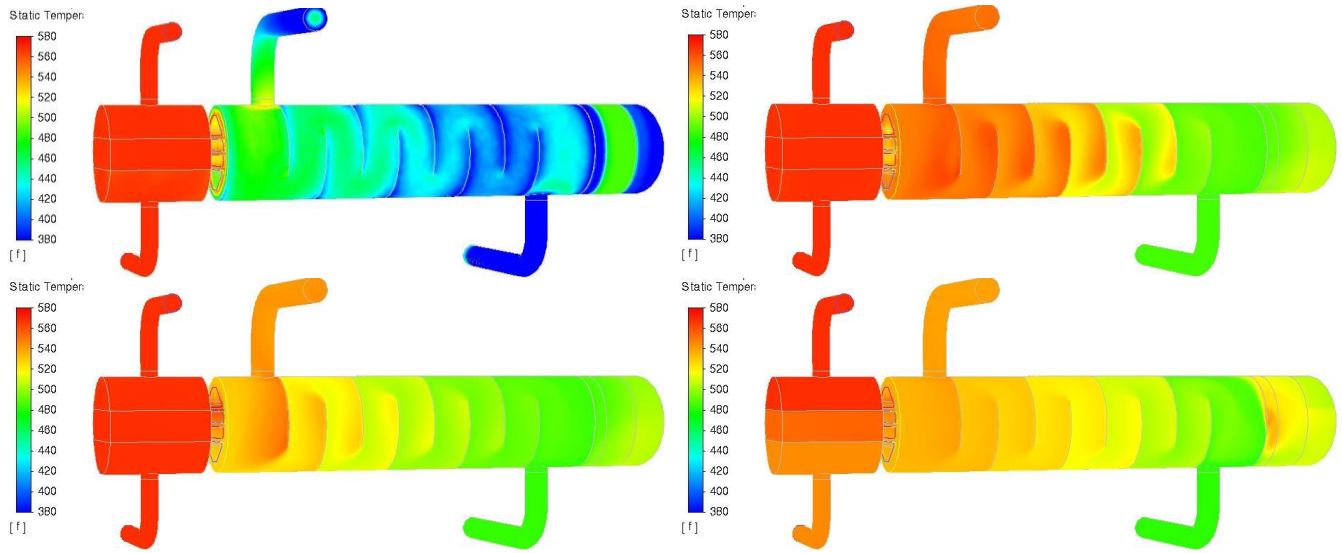


Fig. 9: Wall temperature contour for transition from gas stagnant condition to normal operation (Heating) at (a) 1 second (b) 15 seconds (c) 30 seconds, and (d) 930 seconds. Temperature ranges from approximately 193 °C to 305 °C (380 °F to 580 °F).

4. Conclusion

This paper shows computational fluid dynamics analysis of temperature gradient for a heat exchanger that experienced repeated leaks. The analysis ultimately resulted in global stresses and displacements in the heater train and detailed stresses and displacements in the heater flanges and gaskets under combined structural and thermal loads. The simulated conditions include 5 steady-state and transient operating conditions.

The analysis results yielded the following findings regarding the heater flanges. Thermal expansion (under both steady-state and transient thermal conditions) and pressure load cause loss of bolt load and further reduces gasket contact pressure. Maximum gasket scuffing due to differential radial thermal expansion could result in gasket damage over repeated thermal cycles. These behaviors are cumulative in that their combined effect is the most likely root cause of the repeated heater leaks. Additional potential root causes of the leaks could be: damage to gasket during assembly due to poor technique, poor gasket selection for service leading to gasket failure, incorrect assembly bolt load selection, incorrect application of specified bolt load, and excessive gasket relaxation. The CFD results will be used for further study using finite element analysis (FEA) to clearly identify the effect of gasket type on the heater leaks. The FEA results will be discussed in a future work.

References

- [1] Shah, Ramesh K., and Dusan P. Sekulic. Fundamentals of heat exchanger design. John Wiley & Sons, 2003.
- [2] Fraas, Arthur P. Heat exchanger design. John Wiley & Sons, 1991.
- [3] Yang, J., Fan, A., Liu, W., & Jacobi, A. M. "Optimization of shell-and-tube heat exchangers conforming to TEMA standards with designs motivated by constructal theory." *Energy conversion and management* 78 (2014): 468-476.
- [4] Anderson, John David, and J. Wendt. Computational fluid dynamics. Vol. 206. New York: McGraw-Hill, 1995.
- [5] Pacio, Julio Cesar, and Carlos Alberto Dorao. "A review on heat exchanger thermal hydraulic models for cryogenic applications." *Cryogenics* 51.7 (2011): 366-379.
- [6] Brown, Warren, and David Reeves. "Failure of heat exchanger gaskets due to differential radial expansion of the mating flanges." *ASME-PUBLICATIONS-PVP* 416 (2001): 119-122.
- [7] Wang, B., Varbanov, P. S., Klemeš, J. J., Liu, X., & Yang, W. "Heat integration incorporating leakage risk assessment of heat exchanger networks." *Computers & Chemical Engineering* 145 (2021): 107173.